Specific Contact Resistivity Measurement by a Vertical Kelvin Test Structure

TAN FU LEI, LEN-YI LEU, AND CHUNG LEN LEE

***Abstract*—A vertical Kelvin test structure is used to measure the specific contact resistivity of the Al(1-percent Si)/Si and Al(1-percent Si)/$TiSi_2$/Si contact system. For the vertical test structure, the driving current flows "vertically," thus the current crowdings and sheet resistance effects are eliminated and measurement on the true specific contact resistivity becomes possible. Experimental works show that results obtained by using this vertical structure are closer to the true specific contact resistivities than those obtained by using the conventional six-terminal Kelvin method. It is also found that R_{sd}, the sheet resistance directly underneath the contact pad, is much less than that of the conduction bar without the contact pad. A value of $(1.17 \pm 0.17) \times 10^{-7}\ \Omega \cdot cm^2$ specific contact resistivity is obtained for the Al(1-percent Si)/$TiSi_2$(direct reaction)/Si system.**

I. Introduction

SPECIFIC contact resistivity ρ_c, defined as $(\partial J/\partial V)^{-1}$ for $V \to 0$, is one of the most important parameters in studying interfacial properties of metallization systems. Due to the scalings of semiconductor devices in VLSI, the required specific contact resistivity on contact systems in VLSI is in the order of $10^{-6} \sim 10^{-7}\ \Omega \cdot cm^2$ [1]. Various contact systems and processes [1]–[3] have been studied to give the contact resistance of the above order. However, as the contact resistance is reduced, accurate measurement of the "true" specific contact resistivity becomes more difficult. Many parasitic effects that were negligible previously become significant in determining quantities of the above order.

In measuring the specific contact resistivity, various test structures and methods have been proposed and studied. Among them are: the two-terminal method by Cox and Strack [4], the transfer length (TLM) by Shockley [5], the four-terminal Kelvin method by Cohen *et al.* [6], and the six-terminal Kelvin method by Proctor *et al.* [7]. For the former two methods, large errors will result since the contact resistance is obtained by calculating small differences of large terms. For the latter two Kelvin methods, more accurate, if not exact, measurement of the end contact resistance R_e, or the contact resistance R_c, can be obtained. However, two recent numerical studies [8], [9] of the six-terminal method showed that, for these two types of test structures, the inherent lateral current crowding effects (both horizontal and vertical; see Fig. 1) and the junction sheet resistance effect affect the accuracy of the obtained contact resistance values. The reason for this inaccuracy comes from the fact that, for these two types of test structures, the current flows "horizontally" in a diffused bar while the "vertical" interfacial contact resistance is to be obtained.

Manuscript received September 23, 1986; revised January 26, 1987. This work was supported by the Electronic Research and Service Organization (ERSO), ITRI, Republic of China.

The authors are with the Institute of Electronics, National Chiao Tung University, Hsin Chu, Taiwan, Republic of China.

IEEE Log Number 8613910.

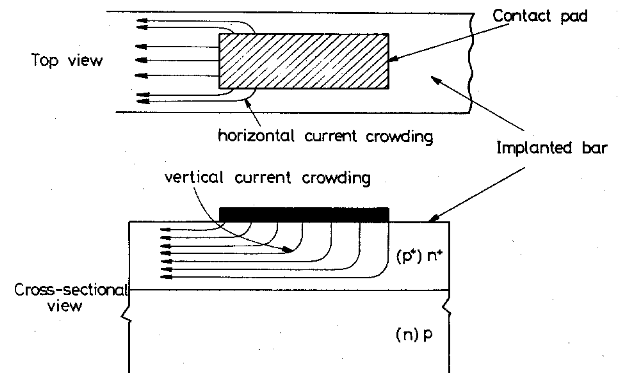

Fig. 1. A top view and a cross-sectional view of a "horizontal" type of test structure to show the horizontal crowding effect and the vertical crowding effect, respectively.

In this paper, a "vertical" Kelvin test structure is presented to measure the "true" specific contact resistivity. For this test structure, the driving current flows "vertically" from the metal contact pad toward the contacted substrate. This eliminates the current crowding effects and the junction sheet resistance effect and makes the determination of the "true" specific contact resistivity possible. Besides, this test structure can be incorporated with the six-terminal test structure and the six-terminal measurement can be performed on the same contact. These two measurement results can be compared to ensure the correctness of measurements. Initial work on this test structure has been reported earlier [10].

This test structure is applied to Al(1-percent Si)/Si and Al(1 percent)/$TiSi_2$/Si contact systems to measure their contact resistances. All data show that this vertical test structure can give better measurement on the true specific contact resistivity. From measured values of specific contact resistivities and also the measured "end" contact resistance from the same test structure R_{sd}, the sheet resistance underneath the contact pad is calculated. It is found that this sheet resistance is much less than that of the conduction bar. Also, a contact resistance of a value of $(1.17 \pm 0.17) \times 10^{-7}\ \Omega \cdot cm^2$, measured by using

0018-9383/87/0600-1390$01.00 © 1987 IEEE

this vertical test structure, has been obtained for the Al(1-percent Si)/$TiSi_2$(direct reaction)/Si system.

II. The Vertical Kelvin Test Structure

Fig. 2(a) shows a cross-sectional view of the vertical Kelvin test structure and Fig. 2(b) shows its corresponding top view. Four masks are used to fabricate this structure. Mask 1 forms the isolation p-n junction. Mask 2 forms the heavily doped conduction bar. Mask 3 opens the contact window, and mask 4 defines the metallization pattern. Compared to the conventional four-terminal or six-terminal test structure, one extra mask step (mask 1) is needed. The driving current I is forced from pad 1 toward the substrate and the voltage is sensed between pads 2 and 3 along the heavily doped conduction bar. The vertical current flow is restricted by an isolation p-n junction. For this structure, it can be seen that the current flows vertically and only through the contact window; hence, the current distribution in the contact region is metallurgically uniform. No vertical and horizontal current crowdings are expected. The contact resistance R_c is thus directly measured with the value of V/I and the specific contact resistivity is $A_c(V/I)$, where A_c is the contact area through which the current passes. Also, the sheet resistance effect on determining the value of ρ_c becomes minimum since it is not at all involved.

In Fig. 2, the six-terminal structure is also incorporated and this has two merits. First, the voltage V can also be sensed between pad pairs 2–4, 2–5, and 2–6. The obtained values can be averaged with that of the pad pair 2–3 to reduce the error introduced by the experiments. Second, as mentioned previously, a six-terminal measurement can be performed on the same contact and the result obtained can be used to compare with that obtained by the vertical Kelvin method to assure the correctness of measurements. Furthermore, in this structure, the "end" contact resistance R_e can also be measured directly. With this measured R_e, and the modified transmission line (MTL) model [11], the "front" contact resistance R_f and the sheet resistance R_{sd} of the heavily doped conduction bar underneath the contact region can be calculated through the following equations [11]:

$$R_e = \left\{[(R_{sd}/W) /\!\!/ (R_s/2\delta)] \times \rho_c/W\right\}^{1/2} / \sinh\left\{[(R_{sd}/W) /\!\!/ (R_s/2\delta)]^{1/2} \times (W/\rho_c)^{1/2} \times d\right\} \tag{1}$$

$$R_f = \left\{[(R_{sd}/W) /\!\!/ (R_s/2\delta)] \times \rho_c/W\right\}^{1/2} / \tanh\left\{[(R_{sd}/W) /\!\!/ (R_s/2\delta)]^{1/2} \times (W/\rho_c)^{1/2} \times d\right\} \tag{2}$$

where $A /\!\!/ B = AB/(A + B)$, d and W are the length and width of the contact region, and δ and R_s are the alignment tolerance and sheet resistance of the conduction bar outside the contact region, respectively.

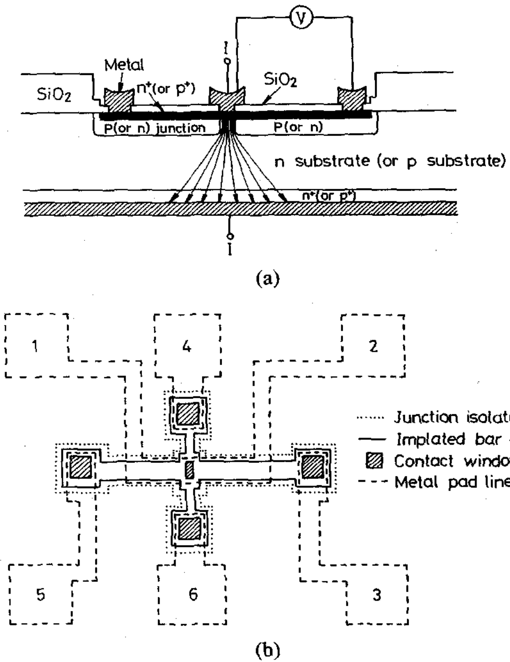

Fig. 2. (a) A cross-sectional view of the proposed vertical Kelvin test structure for measuring the true specific contact resistivity. (b) A top view of the structure. In the figure, the horizontal structure for the six-terminal measurement is also incorporated.

III. Experiments

The test structure of Fig. 2 was fabricated to measure contact resistances. The test structures were formed on n-type substrates of resistivities of 3–5 $\Omega \cdot$ cm. For the measurement of sheet resistance of the conduction bar, the test patterns of the transfer length structure [1] were also formed on the same wafers. Two different contact system, i.e., Al(1-percent Si)/Si and Al(1-percent Si)/$TiSi_2$/Si were used. For the vertical structure test patterns, eight contact sizes (5 μm × 5 μm, 5 μm × 10 μm, 10 μm × 10 μm, 10 μm × 15 μm, 10 μm × 20 μm, 15 μm × 15 μm, 15 μm × 20 μm, and 20 μm × 20 μm) were used for the contact region and the alignment tolerance of the contacts was kept at 10 μm. A set of transfer length test patterns were also fabricated at the same time on the same wafer to measure the sheet resistance of the contact bar. For these transfer length test patterns, six contact windows, each 50 μm × 100 μm in size and spaced apart from 20 to 60 μm in 10-μm increments, were used. The isolation p-n junction was formed by ion implanting BF_2^+ with a dose of $2 \times 10^{13}/cm^2$ and was kept shallow in the subsequent heat treatment to reduce the lateral diffusion. The junction of the n^+ heavily doped conduction bar was also kept shallow by ion-implanting As^+ to reduce the current spreading, which will contribute a measurement error to this test structure, in this region. In our experiments, the depths of the n^+ junctions were from 0.33 to 0.5 μm for $2 \times 10^{15}/cm^2$ to $6 \times 10^{15}/cm^2$ ion doses of As^+ and the junction depths of the p-isolations were 0.7 μm for a $2 \times 10^{13}/cm^2$ ion dose of BF_2^+. To form metallization contacts, for the Al(1-percent Si)/Si

system, Al(1-percent Si) was vacuum-evaporated and deposited on the opened contact window. For the Al(1-percent Si)/$TiSi_2$/Si system, two methods were used. One method was to coevaporate Ti and Si at two respective rates, and the formed film had a Si/Ti ratio of 2. The film was then subjected to an annealing process [12] at 700°C for 15 min in an H_2 ambient. The other method was to evaporate Ti first on wafers and followed by Mo and poly Si in sequence [13]. The formed multilayer structure was then annealed at 700°C in a N_2 ambient. During annealing, Ti reacted with Si to form the $TiSi_2$ film and Si/Mo acted as the protection layer for oxidation [14]. The Si/Mo film was then stripped and Al(1-percent Si) was evaporated to form the Al(1-percent Si)/$TiSi_2$/Si structure. For both methods, a sheet resistance of 3 Ω/□ was obtained for 700-Å Ti film. The back sides of wafers were n^+ diffused and Al metallized. In the measurement, a Keithley 230 programmable current source and a Keithley 619 programmable multimeter were used to provide current driving and to sense voltages, respectively. For each wafer, at least 200 test patterns were measured.

IV. Experimental Results and Discussions

For all the test structures fabricated, the I–V characteristics were linear at current levels from −5 to 0.5 mA. All the contact resistances were measured within these current levels. Fig. 3(a) and (b) shows the log–log plots of the measured contact resistances for two wafers of the Al(1-percent Si)/Si contact system versus the contact area, where R_{cv} and R_{cs} are measured from the vertical structure and the six-terminal structure, respectively. In these figures, straight lines obtained by the least square fitting are also plotted for each set of data. In Fig. 3(a), the slope of the R_{cv} straight line is −1.04, while that of the R_{cs} line is −0.88. In Fig. 3(b), the R_{cv} line has a slope of −0.97 and the R_{cs} has a slope of −0.95. For an ideal contact, the slope should be −1 to satisfy the square law [15]. For both figures, R_{cv} values are closer to the ideal line. Fig. 4(a) and (b) shows similar plots for the contact system of Al(1-percent Si)/$TiSi_2$/Si formed by the coevaporation method and by the direct reaction method, respectively. For both figures, the data points do not give good fits for straight lines. However, the slopes of the R_{cv} lines are always closer to −1 than those of R_{cs} lines. They are −0.89 and −0.82 for R_{cv} and R_{cs}, respectively, in Fig. 4(a) and −0.85 and −0.76 for R_{cv} and R_{cs}, respectively, in Fig. 4(b). The reason for these large discrepancies from the ideal value of −1 in these two figures mainly comes from the severe nonuniformity at the interface for the $TiSi_2$/Si system. (The microscopy observation on the contact area after stripping the contact metal revealed this.) The discrepancy from the ideal value of the direct-reaction method is larger than that of the coevaporation method. This result may be related to the fact that the interface of the former method is rougher than that of the latter. In the above figures, it is also seen that the R_{cv} values are always smaller than the R_{cs} values, and the differences become larger for a larger contact area. This is expected since R_{cv} values do not include the current crowding and the sheet resistance effects. For constant alignment tolerance of the contact, when the contact window is larger, these current crowding and sheet resistance effects become more serious. This phenomenon had also been predicted by [8].

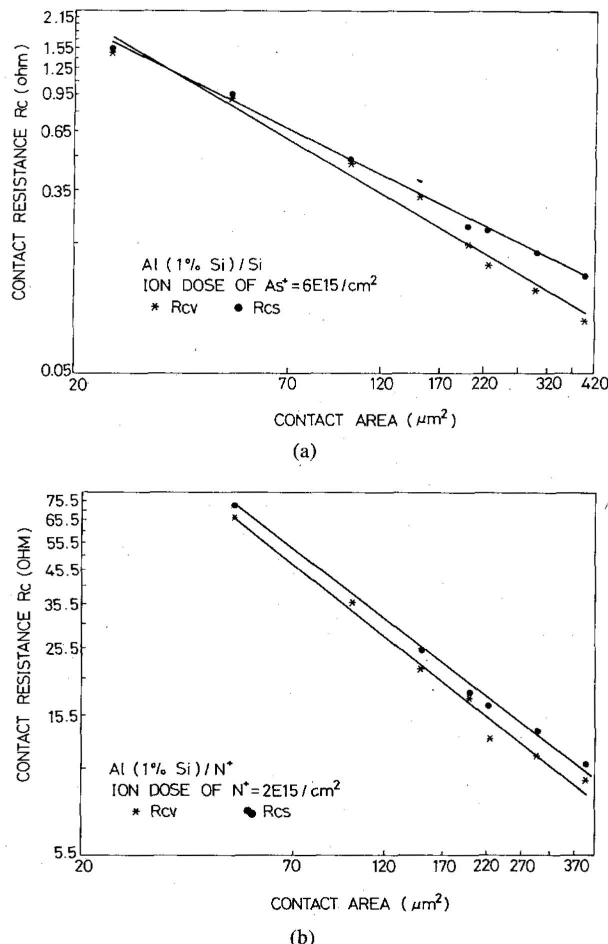

Fig. 3. The contact resistances of Al(1-percent Si)/Si for (a) an ion dose of $As^+ = 6 \times 10^{15}/cm^2$ and (b) an ion dose of $As^+ = 2 \times 10^{15}/cm^2$ are plotted versus the contact area, where R_{cv} and R_{cs} were measured from the vertical structure and six-terminal structure. The straight lines are obtained by the least square fitting method for two sets of measured values, respectively.

The apparent specific contact resistivity of contact systems was measured with the vertical structure (ρ_{cv}) and the six-terminal method (ρ_{cs}) for keeping the contact size constant. Fig. 5(a) and (b) shows plots of ρ_{cv} versus ρ_{cs} with the contact areas being 20 μm × 20 μm and 20 μm × 15 μm, respectively. The various contact resistivities were obtained by implanting various doses of As^+ onto contact windows. For both figures, it is seen that ρ_{cs}/ρ_{cv} deviates more from 1 for smaller specific contact resistivities. Since it has been predicted that ρ_{cs} deviates more from the true value of ρ_c as ρ_c becomes smaller [9], this indicates that ρ_{cv} does give the closer value to the true specific contact resistivity.

Since the end contact resistance R_e can also be mea-

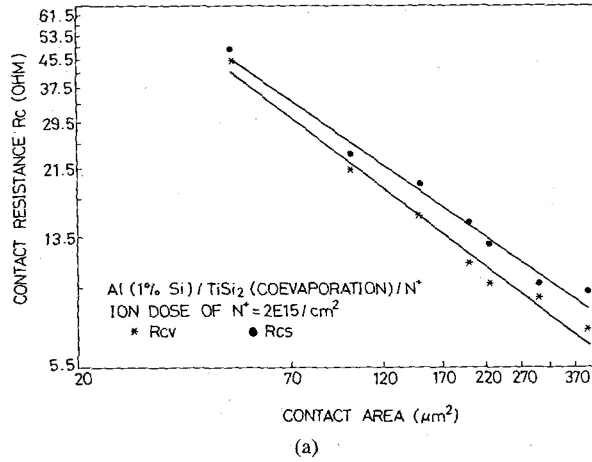

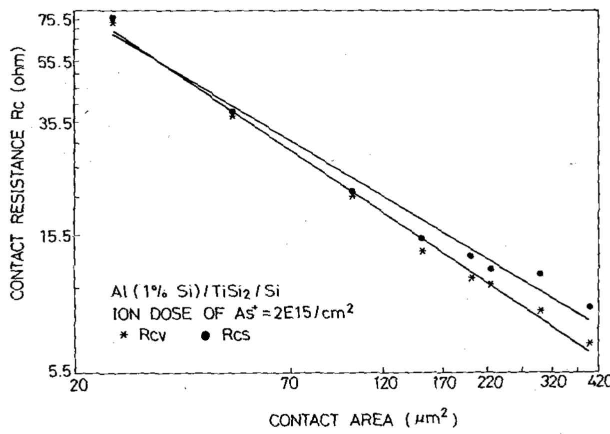

Fig. 4. The contact resistances of Al(1-percent Si)/$TiSi_2$/Si for an ion dose of $As^+ = 2 \times 10^{15}/cm^2$ are plotted versus the contact area, where $TiSi_2$ film was formed by (a) the coevaporation method and (b) the direct reaction method.

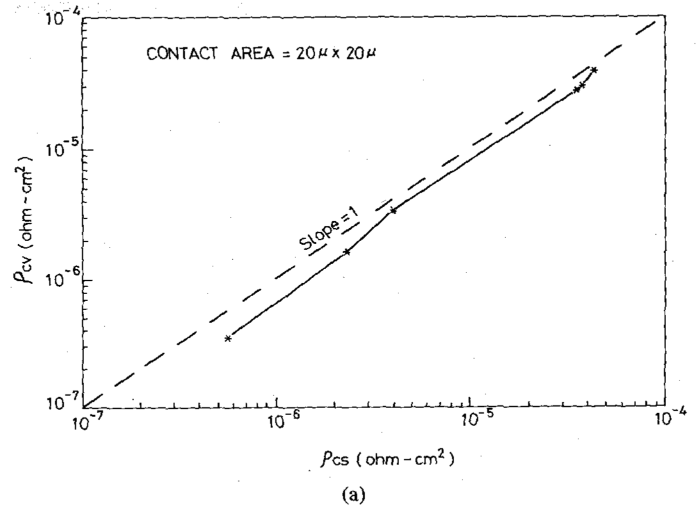

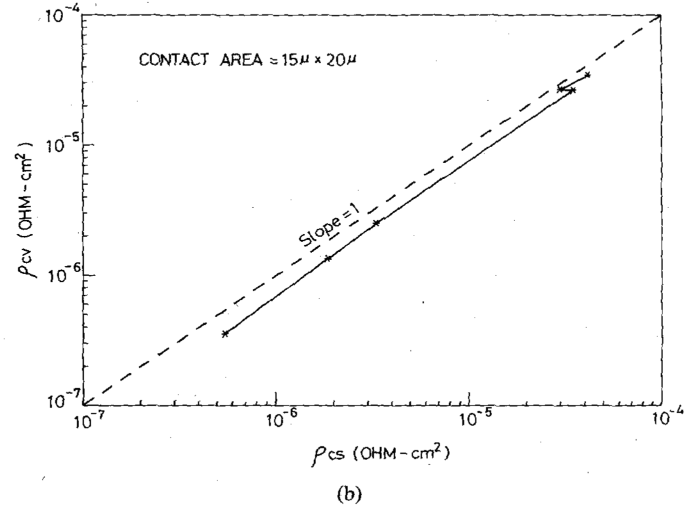

Fig. 5. The apparent specific contact resistivities of contact systems measured from the vertical structure ρ_{cv} are plotted with those measured from the six-terminal structure ρ_{cs}. The contact area was kept constant for (a) $A_c = 20\ \mu m \times 20\ \mu m$ and (b) $A_c = 20\ \mu m \times 15\ \mu m$ during the measurement.

sured from the test structure of Fig. 2, it was measured along with R_c for different contact areas. Fig. 6(a) shows the plots of the measured R_e and R_c values versus contact areas in linear scales for the Al/(1-percent Si)/Si system. In the figure, the experimental R_e values were used to fit (1) to obtain the value for R_{sd}, the sheet resistance underneath the contact pad. In the fittings, R_s was obtained from the separate TLM test structures that were fabricated on the same wafer. For this case, R_s was obtained to be 46.5 $\Omega/\square$ and the derived R_{sd} value was 20.5 $\Omega/\square$. The fitted curve based on (1) for R_e is plotted in the figure as the dotted curve. Also, the obtained R_s and R_{sd} values can be used to compute R_f from (2). In the figure, it is plotted as the solid curve. It is seen that the R_f curve is above the R_c and R_e curves in the figure, as it should be [11], [16]. It is worthwhile to mention that, in obtaining R_{sd} from (1), if ρ_{cs}, instead of ρ_{cv}, was used for ρ_c, the errors in the least square fittings were much larger than that of the case when ρ_{cv} was used. Fig. 6(b) shows the fitted curves, for ρ_{cs} cases with three R_{sd} values. It is seen that even for $R_{sd} = 46.5\ \Omega/\square = R_s$, the computed R_e curve is still above the measured R_{cs} values.

The R_{sd} values obtained with the above method were much less than their corresponding R_s values. Table I compiles the R_{sd} values for five of the contacted wafers in this experiment along with their respective R_s values. For wafers 1 and 3, R_{sd} were even one order of magnitude less than R_s. This result is consistent with that obtained by Reeves and Harrison [17] and Mazer and Lindholm [18].

Finally, the specific contact resistivities, measured by using the vertical Kelvin test structure, for these two metallization systems are plotted versus the surface implanted doses in Fig. 7. In these plottings, the contact areas were assumed to be uniform for the Al(1-percent Si)/$TiSi_2$/Si system during the computation of ρ_c. For both contact systems, ρ_c drops nearly two orders of magnitude when the ion dose increases from $2 \times 10^{15}/cm^2$ to $6 \times 10^{15}/cm^2$. For the Al(1-percent Si)/Si contact, ρ_c is always less than that of the Al(1-percent Si)/$TiSi_2$/Si contact for the same ion dose. For the Al(1-percent Si)/$TiSi_2$(direct reaction)/Si system, a ρ_c value of (1.17

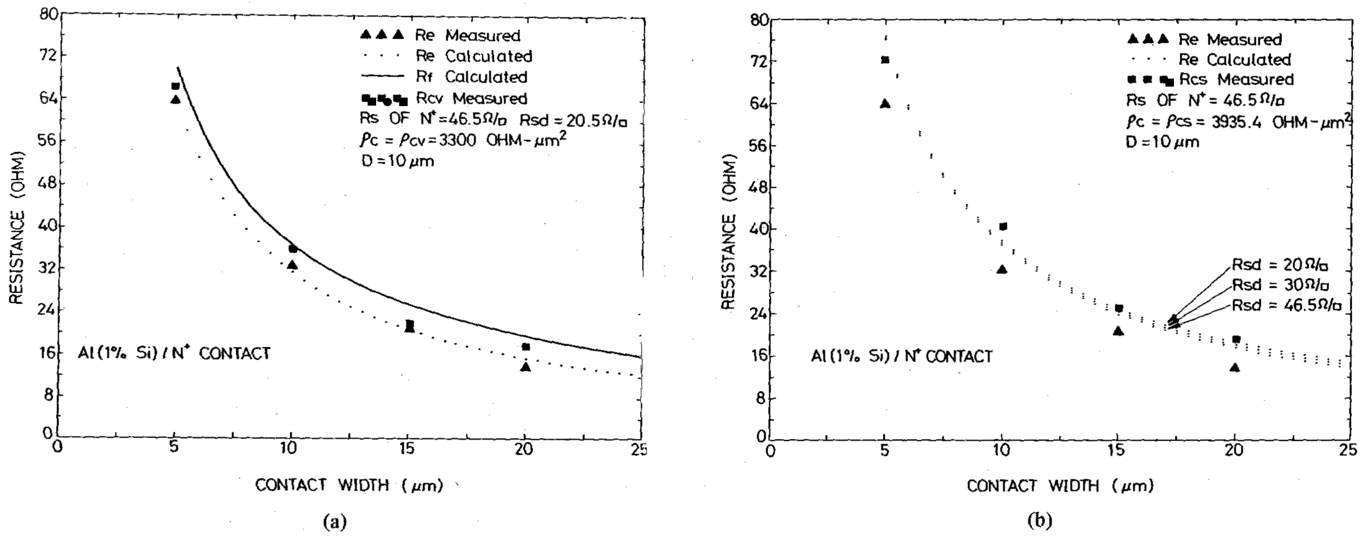

Fig. 6. (a) The measured R_c, R_e and theoretical R_e, R_f obtained from MTL equations with $\rho_c = \overline{\rho_{cv}}$ are plotted with different contact widths. The contact length in this case was kept at 10 μm. (b) $\overline{\rho_{cs}}$, instead of $\overline{\rho_{cv}}$, was used to calculate theoretical R_e and R_f for the same wafer as (a). R_{sd} was varied from 20 to 46.5 $\Omega/\square$ and no good fit between measured R_e and theoretical value can be obtained.

TABLE I
THE MEASURED R_s AND R_{sd} VALUES FOR SOME OF THE FABRICATED WAFERS

Wafer No.	1	2	3	4	5
Contact System	Al(1%Si)/Si	Al(1%Si)/Si	Al(1%Si)/$TiSi_2$/Si direct reaction	Al(1%Si)/$TiSi_2$/Si coevaporation	Al(1%Si)/$TiSi_2$/Si direct reaction
R_{sd} (Ω/□)	1.29	20.5	1.96	9.27	13.3
R_s (Ω/□)	22.67	46.5	26.5	46.5	46.5

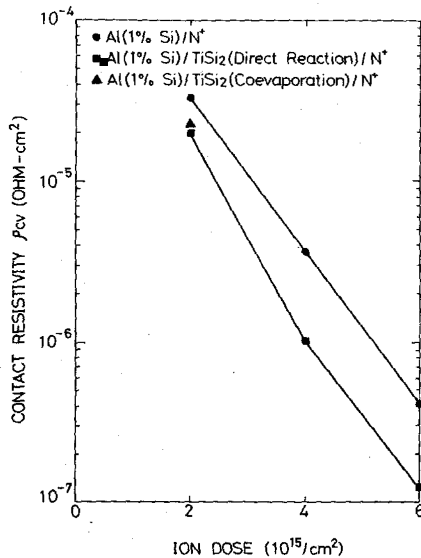

Fig. 7. The specific contact resistivities, measured by a vertical Kelvin test structure, of all the wafers are plotted versus the implanted doses of the conduction bars.

$\pm$ 0.17) $\times$ 10^{-7} $\Omega \cdot cm^2$ for a 5 μm $\times$ 5 μm contact area with an implanted dose of 6 $\times$ $10^{15}/cm^2$ (corresponding to N_D = 1.69 $\times$ $10^{20}/cm^3$) was obtained. This ρ_c value is compatible with the published data of (1.7 $\pm$ 0.2) $\times$ 10^{-7} $\Omega \cdot cm^2$ (measured by the six-terminal method) at the same contact size and N_D = 1.9 $\times$ $10^{20}/cm^3$ [8]. In the experiments, it was also observed that the ρ_c value for the Al(1-percent Si)/$TiSi_2$/Si system obtained by the direct-reaction method was always less than that obtained by the coevaporation method.

It should be mentioned that for this vertical Kelvin test structure, besides the interface nonuniformity, the errors mainly come from the misalignment of the first mask to form the isolation p-n junction and the third mask to open the contact window. When this happens, the current flow is not strictly vertical at the periphery of the contact region. In experiments, it was found that, for some wafers, the R_{cv} as well as the R_{cs} values obtained from one arm of the implanted bar were always larger than those obtained from the other arm. This indicated that a misalignment existed. Hence, averaging the four R_{cv} values obtained by

sensing on pad pairs 2-3, 2-4, 2-5, and 2-6 is a necessity. Other factors for causing errors in this test structure are the lateral diffusion and the depletion width of the isolation p-n junction. However, these errors can be minimized by taking into account the lateral diffusion and the depletion width during the mask design.

V. Conclusions

From results depicted in Figs. 3-7, it can be concluded that the vertical Kelvin test structure does give better measurement on the specific contact resistivity. The current crowding effects and sheet resistance effect that are intrinsically inherent in other "horizontal" test structures are eliminated if the misalignment and the lateral diffusion effects, which technically can be reduced to a minimum, are taken care of for this vertical test structure. If the contact interface is uniform, the measurement on the "true" specific contact resistivity becomes possible.

Also, in this work it was found that R_{sd} is much less than R_s. This confirms the results obtained in [17]. Finally, a specific contact resistivity of the value of $(1.17 \pm 0.17) \times 10^{-7}\ \Omega \cdot cm^2$, measured by the vertical test structure, for the Al(1-percent Si)/$TiSi_2$(direct reaction)/Si system, has been obtained.

References

[1] J. Y.-T. Chen and D. B. Rensch, "The use of refractory metal and electron beam sintering to reduce contact resistance for VLSI," *IEEE Trans. Electron Devices*, vol. ED-30, pp. 1542-1550, Nov. 1983.

[2] S. Swirhum, K. C. Saraswat, and R. M. Swanson, "Contact resistance of LPCVD W/Al and PtSi/W/Al metallization," *IEEE Electron Device Lett.*, vol. EDL-5, pp. 209-211, June 1984.

[3] S. S. Cohen, P. A. Piacente, G. Gildenblat, and D. M. Brown, "Platinum silicide ohmic contacts to shallow junctions in silicon," *J. Appl. Phys.*, vol. 53, no. 12, pp. 8856-8862, Dec. 1982.

[4] R. H. Cox and H. Strack, "Ohmic contacts for GaAs devices," *Solid-State Electron.*, vol. 10, pp. 1213-1218, 1967.

[5] W. Shockley, "Research and investigation of inverse epitaxial UHF power transistors," Air Force Atomic Lab., Wright-Patterson Air Force Base, OH, Rep. Al-TOR-207, Sept. 1964.

[6] S. S. Cohen, G. Gildenblat, M. Ghezzo, and D. M. Brown, "Al-1%Si/Si ohmic contacts to shallow junctions," *J. Electrochem. Soc.*, vol. 129, no. 6, pp. 1335-1338, 1982.

[7] S. J. Proctor, L. W. Linholm, and J. A. Mazer, "Direct measurements of interfacial contact resistance, end contact resistance, and interfacial contact layer uniformity," *IEEE Trans. Electron Devices*, vol. ED-30, pp. 1535-1541, Nov. 1983.

[8] M. Finetti, A. Scorzoni, and G. Soncini, "Lateral current crowding effects on contact resistance measurements in four terminal resistor test patterns," *IEEE Electron Device Lett.*, vol. EDL-5, pp. 524-526, Dec. 1984.

[9] W. H. Loh, K. Saraswat, and R. W. Dutton, "Analysis and scaling of Kelvin resistors for extraction of specific contact resistivity," *IEEE Electron Device Lett.*, vol. EDL-6, pp. 105-108, Mar. 1985.

[10] T. F. Lei, L.-Y. Leu, and C. L. Lee, "A vertical Kelvin test structure for measuring the true specific contact resistivity," *IEEE Electron Device Lett.*, vol. EDL-7, pp. 259-261, Apr. 1986.

[11] I. F. Chang, "Contact resistance in diffused resistors," *J. Electrochem. Soc.*, vol. 117, pp. 368-372, Mar. 1970.

[12] P. Révész, J. Gyimesi, and 'E Zsoldos, "Growth of titanium silicide on ion-implanted silicon," *J. Appl. Phys.*, vol. 54, no. 4, pp. 1860-1864, Apr. 1983.

[13] M.-Z. Lin, private communication.

[14] H. K. Park, J. Sachitano, G. Eiclen, E. Lane, and T. Yamaguchi, "Mo/Ti bilayer metallization for a self-aligned $TiSi_2$ process," *J. Vac. Sci. Technol.*, vol. A2, no. 2, pp. 259-263, April-June 1984.

[15] S. S. Cohen, "Contact resistance and methods for its determination," *Thin Solid Films*, vol. 104, pp. 361-379, 1983.

[16] T. F. Lei, C. L. Lee, J. H. Lin, and L. Y. Liau, "2-D analysis on specific contact resistance based on 4-terminal Kelvin resistor structure," in *Proc. Int. EDMS* (Republic of China), pp. 121-123, 1984.

[17] G. K. Reeves and H. B. Harrison, "Obtaining the specific contact resistance from transmission line model measurements," *IEEE Electron Device Lett.*, vol. EDL-3, pp. 111-113, May 1982.

[18] J. A. Mazer and L. W. Linholm, "An improved test structure and Kelvin-measurement method for the determination of integrated circuit from contact resistance," *J. Electrochem. Soc.*, pp. 440-443, Feb. 1985.

*

Tan Fu Lei was born in Keelung, Taiwan, Republic of China, on September 17, 1944. He received the B.S. degree in electrical engineering from National Cheng Kung University, Tainan, Taiwan, in 1967 and the M.S. and Ph.D. degrees in electronic engineering from National Chiao Tung University, Hsinchu, Taiwan, in 1970 and 1979, respectively.

From 1970 to 1972, he was with the Fine Products Microelectronics Corporation, Taiwan, as an Engineer working on the fabrication of small-signal transistors. From 1980 to 1982, he was the Plant Manager of Photronic Corporation, Taiwan, (now Silitek Corporation). Since 1983, he has been an Associate Professor in the Department of Electronics Engineering and the Institute of Electronics, National Chiao Tung University. During 1984 to 1986, he was the Director of the Semiconductor Research Center, National Chiao Tung University. His research interests are semiconductor devices and optoelectronics.

*

Len-Yi Leu was born on June 14, 1961, in Taiwan, Republic of China. He received the B.S. degree in electrophysics in 1983 and the M.S. degree in electronics, both from National Chiao Tung University. He is currently working toward the Ph.D. degree at the University of Southern California, Los Angeles. His research concerns the modeling of heterojunction interface characteristics.

His research interests include semiconductor devices, especially optoelectronic devices, and MOS and CMOS devices in VLSI applications.

*

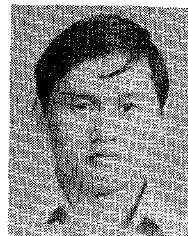

Chung Len Lee (S'71-M'81) was born in 1946 in Hu-Pei, China. He received the B.S. degree in electrical engineering from the National Taiwan University, Taiwan, Republic of China, in 1968, and the M.S. and Ph.D. degrees in electrical engineering from Carnegie-Mellon University, Pittsburgh, PA, in 1971 and 1975, respectively.

In 1975, he joined National Chiao Tung University as a faculty member, engaging in research on various topics on optoelectronics, semiconductor devices, integrated circuits, and processes. He has published more than 50 papers in the above areas. Presently, he is a Professor in the Department of Electronics Engineering at National Chiao Tung University.

Dr. Lee is a member of Phi Kappa Phi and Phi Tau Phi.